Miller, J. F. A. P., Sprent, J., Basten, A., Warner, N. L., Breitner, J. C. S., Rowland, G., Hamilton, J., Silver, H., & Martin, W. J. (1971) *J. Exp. Med. 134*, 1266.
Morrison, M., & Bayse, G. S. (1970) *Biochemistry 9*, 2995.
Ottolenghi, A. C. (1969) *Methods Enzymol. 14*, 188.
Passwell, J. H., Dayer, J. M., & Merler, E. (1979) *J. Immunol. 123*, 115.
Perlman, P., Perlman, J., & Wigzell, H. (1972) *Transplant. Rev. 13*, 91.
Ramasamy, R. (1976) *Immunochemistry 13*, 705.
Record, M., Lloverao, J., Ribes, G., & Douste-Blazy, L. (1977) *Cancer Res. 37*, 4372.
Resch, K., Faber, E., Odenthal, J., & Fischer, H. (1971) *Eur. J. Immunol. 1*, 162.
Revillard, J. P., Samarut, C., Cordier, G., & Brochier, J. (1975) *INSERM Symp. No. 1*, 171.
Robertson, A. F., & Land, W. E. M. (1962) *Biochemistry 1*, 804.
Rock, C. O., & Snyder, F. (1975) *J. Biol. Chem. 250*, 6564.
Shimojo, T., Abe, M., & Ohta, M. (1974) *J. Lipid Res. 15*, 525.
Suzuki, T., Sadasivan, R., Wood, G. W., & Bayer, W. L. (1980) *Mol. Immunol. 17*, 491.
Suzuki, T., Taki, T., Hachimine, K., & Sadasivan, R. (1981) *Mol. Immunol. 18*, 1.
Sweeley, C. C. (1969) *Methods Enzymol. 14*, 254.
Thoenes, J., & Stein, H. (1979) *J. Exp. Med. 150*, 1049.
Thorell, J. I., & Johansson, B. OT. (1971) *Biochim. Biophys. Acta 251*, 363.
Uhr, J. W., & Möller, G. (1968) *Adv. Immunol. 8*, 81.
Uki, J., Young, C. A., & Suzuki, T. (1974) *Immunochemistry 11*, 729.
Vane, J. R. (1976) *Adv. Prostaglandin Thromboxane Res. 2*, 791-801.
Weber, K., & Osborn, M. (1969) *J. Biol. Chem. 244*, 4406.

Raman Spectroscopic Study of the Interactions of Dimyristoyl- and 1-Palmitoyl-2-oleoylphosphatidylcholine Liposomes with Myelin Proteolipid Apoprotein†

Françoise Lavialle‡ and Ira W. Levin*

ABSTRACT: Recombinants of dimyristoylphosphatidylcholine (DMPC) and 1-palmitoyl-2-oleoylphosphatidylcholine (POPC) with myelin proteolipid apoprotein prepared in an aqueous medium were investigated by vibrational Raman spectroscopy. Peak height intensity parameters, involving vibrational transitions in both the 3000-cm^{-1} acyl chain methylene carbon–hydrogen (C–H) stretching mode region and the 1100-cm^{-1} carbon–carbon (C–C) stretching mode region, were used to construct temperature profiles reflecting bilayer inter- and intrachain order–disorder processes. For liposomes reconstituted with DMPC, the gel–liquid-crystalline phase transition T_m, monitored by the C–C stretching mode indices, is depressed from 23 °C for the pure system to 12 °C and broadened from less than 1 °C to ~9 °C. On completion of the phase transition at 15 °C, the intramolecular chain disorder is substantially greater compared to that of the pure bilayer form. In addition, no further development of gauche conformers along the chain is apparent as the temperature increases. For the temperature profile derived from the C–H stretching region parameters of DMPC, the phase transition temperature is shifted from 23 to 11 °C. The intermolecular disorder in both the gel and liquid-crystalline states is significantly greater in the recombinant systems in comparison to that in the pure liposomes. Temperature profiles obtained for recombinants prepared with unsaturated phospholipid bilayers (POPC) indicate that the apoprotein only slightly perturbs the inter- and intramolecular parameters describing the lipid matrix. For assessment of the rather different perturbations of the apoprotein on bilayers containing either saturated or unsaturated acyl chains, the pure DMPC and pure POPC temperature profiles are compared by matching the curves to the same relative temperature with respect to their values for T_m. For the liquid-crystalline state, the POPC bilayers possess a greater population of gauche rotamers along the chain, although the lateral chain order is increased in the unsaturated bilayer compared to that of the saturated DMPC system. The increased intermolecular disorder exhibited by the pure and reconstituted DMPC systems is discussed in terms of the diffusion properties exhibited by saturated and unsaturated lipid matrices. Within the precision of the Raman experiment, no evidence on the vibrational time scale exists for a boundary lipid involving the aqueous solution of the apoprotein in either the saturated or unsaturated bilayer assembly. Finally, observed differences in the Raman temperature profiles obtained from reconstituted liposomes involving the apoprotein prepared from either organic or aqueous media are discussed.

For characterization of the response of lipid bilayer structures to intrinsic membrane components, recombinants of the myelin proteolipid apoprotein, or Folch-Pi apoprotein, with lecithin dispersions have provided tractable lipid–protein systems for a variety of spectroscopic, X-ray diffraction, and calorimetric studies (Verma et al., 1980; Curatolo et al., 1978, 1977; Boggs & Moscarello, 1978; Boggs et al., 1977, 1976). For example, recent calorimetric observations indicate that phosphatidic acid, phosphatidylglycerol, and phosphatidylserine exhibit preferential binding of the hydrophobic apoprotein (Boggs et

† From the Laboratory of Chemical Physics, National Institute of Arthritis, Metabolism and Digestive Diseases, National Institutes of Health, Bethesda, Maryland 20205. *Received June 2, 1980.*
‡ F.L. is on leave from INSERM, Laboratoire des Etats Liés Moléculaires, Paris, France.

al., 1977), although no dependence upon fatty acid chain length in the C-14 to C-18 range was discerned for the membrane protein (Boggs & Moscarello, 1978). Further, it was suggested that lipids with unsaturated trans fatty acid chains, such as dielaidoylphosphatidylcholine, interact less favorably with the apoprotein than saturated lipids (Boggs & Moscarello, 1978). Comparisons of the effects of the proteolipid apoprotein on saturated and unsaturated bilayer lipids were made by Curatolo et al. (1978) in Raman spectroscopic studies involving recombinants with dimyristoylphosphatidylcholine (DMPC) and egg yolk phosphatidylcholine (EYPC) bilayers. In particular, both spectra and order parameters, based upon acyl chain C–C stretching mode intensities, indicate that the bilayer matrix for the apoprotein–DMPC recombinants exhibits a greater population of acyl chain gauche conformers in the gel state and a smaller population of gauche conformers in the liquid-crystalline state than for DMPC bilayers alone (Curatolo et al., 1978). For the EYPC bilayers, which are composed of unsaturated chains, the profiles for the recombinants derived from acyl chain C–H stretching parameters display a more complicated temperature behavior than that for the pure DMPC system (Curatolo et al., 1978). In this case the apoprotein both broadens the main gel–liquid-crystalline phase transition and induces a second high-temperature discontinuity in the temperature profile (Curatolo et al., 1978). For dioleoylphosphatidylcholine bilayers, the Raman spectroscopic report of Verma et al. (1980) notes that the proteolipid apoprotein also broadens the −22 °C main transition and induces a second broad transition at ~1 °C.

In several studies stressing lipid chain dynamics through nuclear magnetic resonance (NMR) techniques, it was observed that the myelin proteolipid apoprotein only slightly increases the disorder and mobility of the hydrocarbon chains for both DMPC and DPPC (dipalmitoylphosphatidylcholine) bilayers above their respective gel–liquid-crystalline phase transition temperatures (Rice et al., 1979a; Oldield et al., 1978). Further, no evidence was found on the ^2H NMR time scale for a class of ordered, less mobile, boundary lipids about the apoprotein (Rice et al., 1979a; Oldfield et al., 1978). The disordering effects of the apoprotein upon the DMPC bilayer lipids were also observed below the phase transition (Rice et al., 1979a; Oldfield et al., 1978). In extending their NMR studies to bilayer systems containing unsaturated acyl chains, Rice et al. (1979b) observed that cytochrome oxidase, an intrinsic membrane component, induces analogous bilayer effects as the Folch-Pi apoprotein in DMPC multilayers (Rice et al., 1979a). In particular, bilayers composed of 1-palmitoyl-2-oleoylphosphatidylcholine (POPC) exhibit a small increase in hydrocarbon chain disorder, compared to pure POPC bilayers, on incorporating the oxidase within the multilayer assembly (Rice et al., 1979b; Seelig & Seelig, 1978).

In this communication we apply vibrational Raman spectroscopic techniques to bilayer systems containing an intrinsic membrane component in an effort to clarify the structural reorganizations occurring within a lipid matrix comprised of either a saturated or unsaturated chain assembly. In particular, we examine the Raman spectral data determined for recombinants of the Folch-Pi apoprotein with DMPC and POPC multilayer dispersions. Although the myelin proteolipid apoprotein may be obtained in soluble form from either organic solvents or aqueous solutions, the structural studies described above were performed by adding the appropriate lipids to the organic solution of the apoprotein. Since significant conformational and molecular weight differences arise for the apoprotein depending upon the solvent system used in its preparation (Sherman & Folch-Pi, 1970; Nicot et al., 1973; Lees et al., 1979; Nguyen Le et al., 1976; Lavialle et al., 1979), we examine the vibrational data for the reconstituted bilayer systems which specifically incorporated the apoprotein prepared in aqueous medium. These spectral data indicate that this form of the apoprotein induces substantially different bilayer effects depending upon the degree of unsaturation within the hydrophobic region of the lipid matrix.

Experimental Section

High-purity samples of 1,2-dimyristoyl-L-α-phosphatidylcholine (DMPC) and 1-palmitoyl-2-oleoyl-L-phosphatidylcholine (POPC) were obtained commercially from Sigma Chemical Co. and from Supelco, Inc., respectively. The Folch-Pi proteolipid was extracted from bovine white matter (Folch-Pi & Lees, 1951) and delipidated by petroleum ether precipitation and acidic dialysis, as previously described (Nicot et al., 1973). Neutral dialysis was first performed for 2 days in order to equilibrate the apoprotein in chloroform–methanol [2:1 (v/v)] mixtures. The apoprotein in this form was transferred to aqueous solution by the method of Sherman & Folch-Pi (1970).

In forming lipid multilayer recombinants with the Folch-Pi apoprotein, either anhydrous DMPC or POPC was added to the aqueous protein solution in the presence of 2-chloroethanol [water–2-chloroethanol, 3:1 (v/v)] to yield a final lipid/protein molar ratio of 340:1 (9.5 wt % apoprotein). The molar ratios are based on an apoprotein molecular weight of 25 000 (Nicot et al., 1973; Chan & Lees, 1974). The lipid–protein samples were then evacuated under vacuum at 10^{-5} torr for approximately 48 h in order to eliminate all traces of solvent. Newly hydrated samples were mechanically agitated for 10 min and incubated at 35 °C for 1 h before being transferred to glass capillaries, 1.5-1.8-mm diameter, for obtaining Raman spectra.

Vibrational Raman spectra were recorded with a Spex Ramalog 6 spectrometer equipped with a set of plane holographic gratings. A Coherent Model CR-3 argon ion laser, delivering 100 mW to the sample at 514.5 nm, served as the excitation source. The spectral resolution was of the order of 5 cm^{-1}; spectral frequencies, calibrated with atomic argon lines from a Geissler-type tube and plasma lines from the laser (Craig & Levin, 1979), are reported to ±2 cm^{-1}. Capillaries containing the bilayer samples were placed within a holder that was thermostatically controlled to ±0.05 °C. Temperatures were monitored by a copper–constantan thermocouple inserted into the holder adjacent to the capillary. The heating curves proceeded from low to high temperatures to obtain temperature profiles for the lipid dispersions. After equilibration of the samples at each temperature for ~15 min, Raman spectra were acquired by using a Nicolet NIC-1180 data system interfaced to the spectrometer. Both the 2800–3100-cm^{-1} C–H and the 990–1200-cm^{-1} C–C stretching regions were scanned at rates of 1 cm^{-1}/s by using signal-averaging techniques. For the more intense 2800–3100-cm^{-1} interval, 5 scans were sufficient for the DMPC- and POPC–apoprotein recombinants, while 15–20 scans were required for the 990–1200-cm^{-1} region for the bilayer–apoprotein dispersions. Significantly fewer scans in each region were required for the pure bilayer samples. Temperature profiles were constructed from original, unsmoothed spectra from peak height intensities for the I_{2940}/I_{2885} interchain disorder–order parameters and the I_{1090}/I_{1130} intramolecular gauche–trans isomerization parameters. Representative spectra for DMPC–apoprotein recombinants for the C–C and C–H stretching regions are shown in Figures 1 and 2, respectively. As a consequence of the relatively high lipid/protein ratios used, no corrections to the observed signal

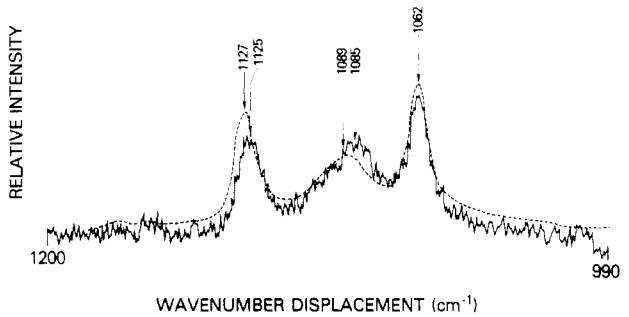

FIGURE 1: Raman spectra of dimyristoylphosphatidylcholine (DMPC)–Folch-Pi apoprotein liposomes in the 1100-cm^{-1} region at 10 °C. The solid line represents a system comprising a 340:1 lipid/protein mole ratio, while the dashed line represents the pure DMPC bilayer system.

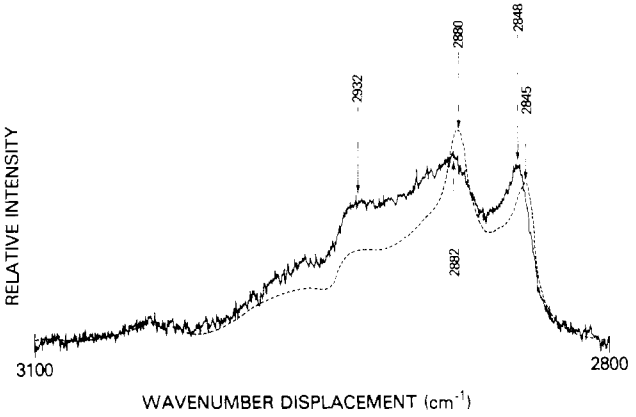

FIGURE 2: Raman spectra of dimyristoylphosphatidylcholine (DMPC)–Folch-Pi apoprotein liposomes in the 2900-cm^{-1} region at 11 °C. The solid line represents a system composed of a 340:1 lipid/protein mole ratio, while the dashed line represents the contour for the pure DMPC bilayer system.

due to protein contributions were required.

Results and Discussion

The spectral intervals that reflect the intramolecular and intermolecular order of the hydrocarbon chains forming the bilayer matrix are respectively the 1000–1200-cm^{-1} skeletal C–C stretching mode region and the 2800–3000-cm^{-1} methylene C–H stretching mode interval. Figures 1 and 2 illustrate the effects of the Folch-Pi apoprotein, in a 340:1 lipid/protein molar ratio, on the acyl chain C–C and C–H stretching modes characteristic of the DMPC gel-state bilayers at 10 and 11 °C, respectively. The pure DMPC bilayer spectrum, represented by the dotted line in Figure 1, displays three features assigned to C–C stretching modes at 1127, 1089, and 1062 cm^{-1}. For the pure gel state the spectral frequencies and intensity distributions in this interval imply an arrangement of highly ordered acyl chains with about one gauche C–C bond per chain located toward the center of the bilayer (Yellin & Levin, 1977a,b). On introduction of the apoprotein within the bilayer, the two higher frequency components exhibit frequency shifts to 1125 and 1085 cm^{-1}, as well as relative intensity readjustments. As we shall discuss below, the peak height intensity ratios observed after the addition of the apoprotein indicate that at 10 °C the intramolecular chain disorder reflects a lipid bilayer whose hydrocarbon chains are halfway through their gel–liquid-crystalline phase transition. Thus, the decrease in intensity at 1125 cm^{-1} coupled with an increase in intensity at 1085 cm^{-1} (Figure 1) indicates an increase in the number of gauche conformers, at the expense of all-trans segments, along the hydrocarbon chains (Spiker & Levin, 1976).

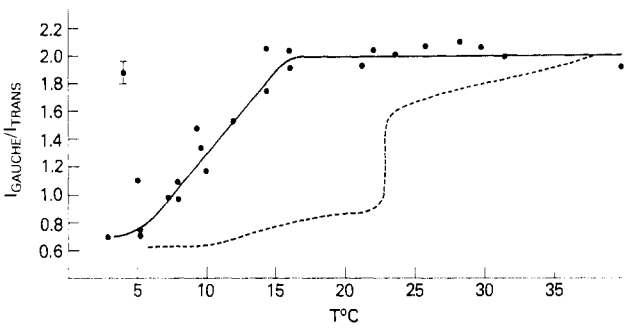

FIGURE 3: Temperature profile for the DMPC–apoprotein recombinant using the I_{1100}/I_{1130} (I_{gauche}/I_{trans}) peak height intensity ratios as indices. (●) represents the profile for a 340:1 DMPC/apoprotein mole ratio, while the dashed line represents the profile for the pure DMPC bilayer assembly.

Significant alterations in spectral intensity arise in the acyl chain C–H stretching region as the chain–chain intermolecular interactions are modified by the addition of the apoprotein. Figure 2 records frequency shifts for the methylene symmetric and antisymmetric C–H stretching modes from 2845 and 2880 cm^{-1}, respectively, in the pure DMPC gel phase to 2848 and 2882 cm^{-1} for the recombinant at 11 °C. The intensity increase for the 2932-cm^{-1} feature reflects, in part, the appearance of an underlying manifold of infrared active methylene asymmetric stretching modes (Bunow & Levin, 1977).

Temperature Profiles for the DMPC–Apoprotein Bilayer Complexes. Temperature profiles for the hydrocarbon C–C stretching region, presented in Figure 3 for both the pure DMPC bilayer and the DMPC–apoprotein recombinant, were constructed from the intensity ratios I_{gauche}/I_{trans}, where I_{gauche} and I_{trans} represent the peak height intensities for the 1085- and 1125-cm^{-1} transitions, respectively. As shown in the figure, pure DMPC bilayers undergo a sharp, primary gel–liquid-crystalline phase transition at 23 °C with a smaller order–disorder pretransition occurring at 12 °C. The intrusion of the apoprotein into the hydrophobic region of the bilayer depresses the gel–liquid-crystalline transition temperature to ~10 °C, with the phase transition interval broadened to ~9 °C, as compared to about a 1 °C interval for pure DMPC multilayers. For the DMPC reference system the population of gauche conformers continues to increase in the liquid-crystalline region from 24 to 35 °C, as reflected by the increase in I_{gauche}/I_{trans} from 1.6 to ~2.0 for this temperature range. In contrast, once the liquid-crystalline region is attained for the apoprotein recombinants, no further development of gauche conformers along the chain is apparent in the 15–35 °C range. On completion of the phase transition at 15 °C, the intramolecular chain disorder in the liquid-crystalline state for the reconstituted DMPC multilayers is substantially greater in comparison to that of the liquid-crystalline form for the pure bilayers; that is, the I_{gauche}/I_{trans} ratio for the DMPC–apoprotein liposomes is 2.0 compared to 1.6 for the pure multilayers at 24 °C.

In a recent Raman spectroscopic study involving the interaction of melittin, a polypeptide consisting of 26 amino acids with DMPC bilayers, the temperature profile, based upon the chain C–C stretching region for the reconstituted liposomes, displayed a second order–disorder transition at higher temperatures relative to the primary gel–liquid-crystalline phase transition (Lavialle et al., 1980). This second thermal transition was associated with the fluidization of immobilized boundary lipids at the polypeptide–lipid interface within the bilayer. As shown in Figure 3, no analogous behavior is seen, within the precision of the present experiment, for the re-

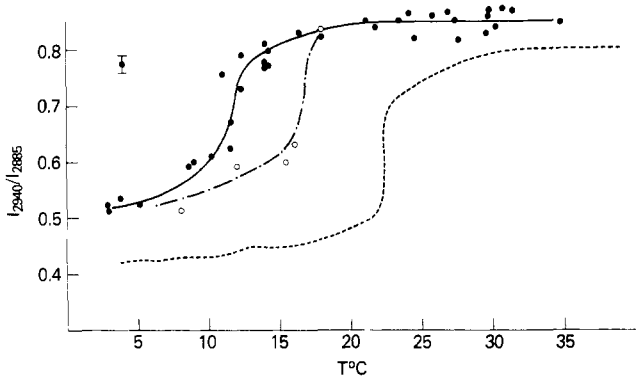

FIGURE 4: Temperature profiles for DMPC–apoprotein recombinants using the I_{2940}/I_{2885} peak height intensity ratios as indices. (●) and (○) represent the profiles for a 340:1 DMPC/apoprotein mole ratio (see the text), while the dashed line represents the profile for the pure DMPC bilayer assembly.

constituted DMPC–apoprotein liposomes. Evidence for a small population of more ordered lipid within a somewhat disordered lipid matrix for the DMPC–apoprotein multilayers at 10 °C, however, is observed in the spectrum shown in Figure 1. In particular, the broad shoulder at ~1092 cm^{-1}, which does not appear in disordered, pure DMPC bilayers, implies the existence of ordered lipid chains within the lipid dispersion containing the apoprotein.

In the Raman study of recombinants in a lipid/apoprotein molar ratio of 680:1 for DMPC with an apoprotein preparation delipidated with organic solvents (Curatolo et al., 1978), evidence was observed for an increase in the number of gauche conformers below the phase transition; however, the liquid-crystalline state was more ordered than that for pure DMPC multilayers. This behavior for the liquid-crystalline state is in contrast to that observed here in that the apoprotein dissolved in the aqueous medium significantly disorders the liquid-crystalline state. The 10 °C depression in the gel–liquid-crystalline phase transition temperature T_m observed in the present work is compared to the Curatolo et al. (1978) study in which essentially no depression in T_m was observed. The dramatic difference in the extent to which the apoprotein perturbs the bilayer in the two studies probably arises from an increase in molecular weight (vide infra) which occurs during the transfer of the apoprotein from an organic medium to an aqueous solution (Nicot et al., 1973; Nguyen Le, 1976; Lavialle et al., 1979).

Figure 4 presents the temperature profiles based on the peak height intensities for the methylene CH_2 antisymmetric stretching modes at 2940 and 2885 cm^{-1}. As the ratio I_{2940}/I_{2885} increases, the DMPC bilayer is presumed to undergo a disordering of the hydrocarbon chain lattice (Yellin & Levin, 1977b; Gaber & Peticolas, 1977). As observed for the C–C stretching region temperature profile, T_m is depressed from 23 to 10–11 °C in the presence of apoprotein. The midpoint of the induced phase transition corresponds to the region for the pretransition endotherm for the pure bilayers (see Figures 3 and 4). Following completion of the phase transition, the DMPC–apoprotein recombinants exhibit a significantly greater intermolecular disorder in comparison to the pure bilayers. While the gel-state intramolecular chain disorder for the recombinant is about the same as that exhibited by the pure bilayer (Figure 3), the intermolecular disorder (Figure 4) assumed by the recombinant in the gel state is much greater than that for the pure dispersion. The apoprotein thus distorts the lipid lattice arrangement in the gel phase without inducing a significant increase in gauche chain conformers.

Figure 4 also displays a second temperature profile, marked by a dash–dot line with approximately the same characteristics as the profile discussed above except that T_m appears at a slightly higher temperature, ~16.5 °C. This profile was obtained after refrigerating the DMPC–apoprotein recombinants at 4 °C for 5 days as compared to a 21-day refrigeration period for the sample yielding T_m at 10.5 °C. The increased lipid perturbation may reflect either a modification of physical properties of the apoprotein or the existence of metastable states for the apoprotein–lipid bilayer complex.

Temperature Profiles for the POPC–Apoprotein Bilayer Complexes. Temperature profiles in Figures 5 and 6 demonstrate the effects of the Folch-Pi apoprotein on the melting behavior of POPC bilayers. Figure 5, the C–C stretching region profile, indicates that the transition temperature is broadened slightly and depressed in the POPC–apoprotein complex to approximately –3 from –1.5 °C for the pure bilayer

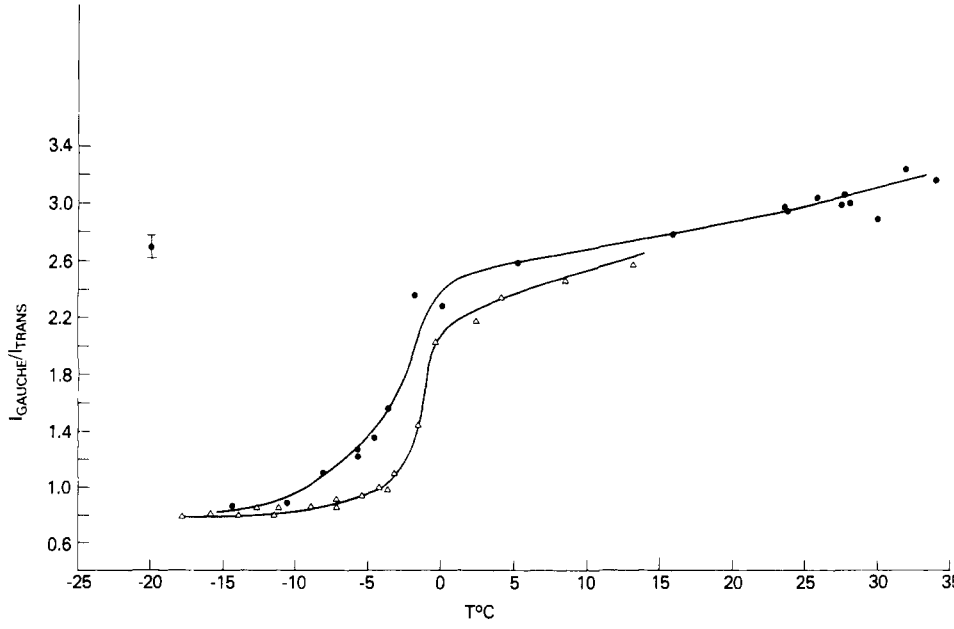

FIGURE 5: Temperature profile for the POPC–apoprotein recombinant using the I_{1100}/I_{1130} peak height intensity ratios as indices. (●) represents the profile for a 340:1 POPC/apoprotein mole ratio, while (△) represents the profile for the pure POPC bilayer system.

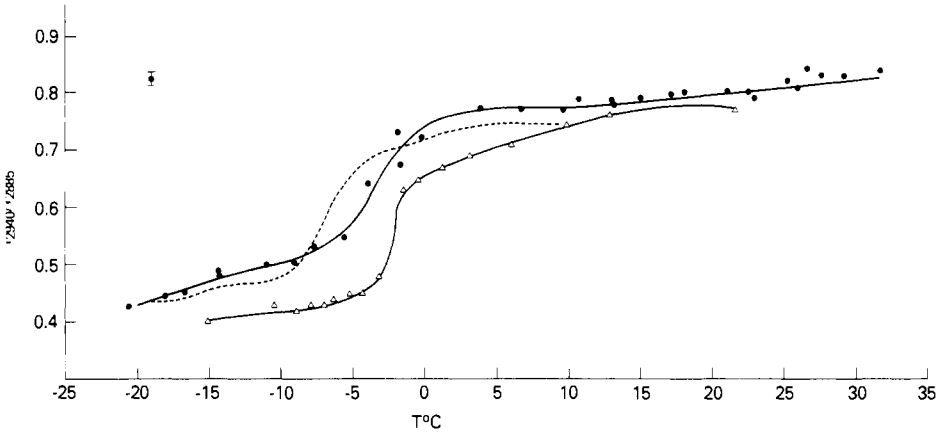

FIGURE 6: Temperature profile for the POPC–apoprotein recombinant using the I_{2940}/I_{2885} peak height intensity ratios as indices. (●) represents the profile for a 340:1 POPC/apoprotein mole ratio, while the dashed line and (△) represent profiles for the pure POPC bilayer system.

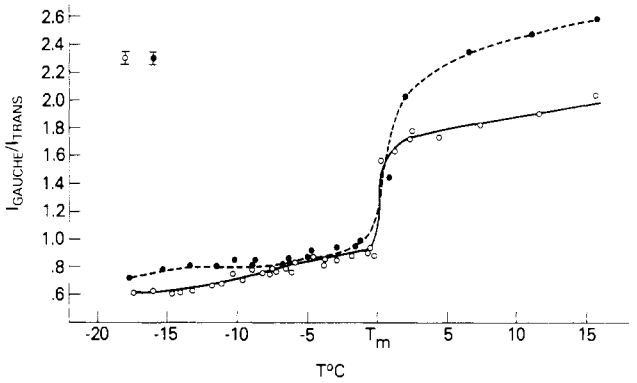

FIGURE 7: Comparisons of the temperature profiles of POPC and DMPC using I_{gauche}/I_{trans} peak height intensity ratios as markers. The abscissa represents the temperature interval from T_m, the gel–liquid-crystalline phase transition temperature. The solid line (○) represents the profile for the DMPC bilayers, while the dashed line (●) represents the profile for the POPC bilayers.

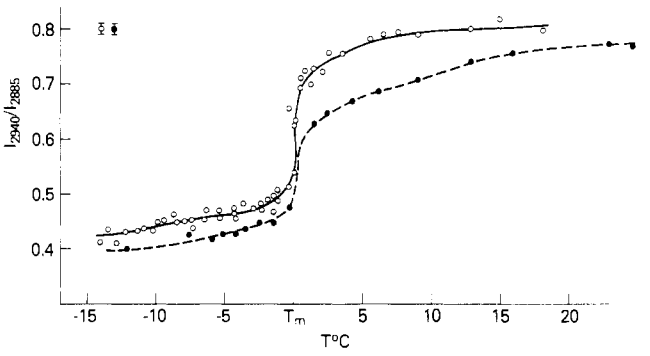

FIGURE 8: Comparisons of the temperature profiles of POPC and DMPC using I_{2940}/I_{2885} peak height intensity ratios as markers. The abscissa represents the temperature interval from T_m, the gel–liquid-crystalline phase transition temperature. The solid line (○) represents the profile for the DMPC bilayers, while the dashed line (●) represents the profile for the POPC bilayers.

form. The apoprotein–lipid system exhibits a somewhat greater intramolecular disorder after melting compared to pure POPC multilayers.

The temperature profiles in Figure 6, representative of the C–H stretching region, illustrate an additional complexity associated with POPC bilayers, namely, the existence of metastable forms as demonstrated by T_m values of −2.5 and −7 °C for the pure POPC liposomes. A detailed discussion of the temperature characteristics of POPC bilayers will be presented at another time. We note, however, that the apoprotein-containing bilayers exhibit a T_m at −3.5 °C with the attendant intermolecular disorder in the liquid-crystalline state being greater than that for the pure bilayer.

Comparison of the DMPC and POPC Gel–Liquid-Crystalline Phase Transition Characteristics. As an aid in assessing the rather different perturbations of the Folch-Pi apoprotein on bilayers containing either saturated or unsaturated hydrocarbon chains, we compare the DMPC and POPC temperature profiles directly in Figures 7 and 8, by matching the curves to the same relative temperature with respect to their values for T_m. Although the monounsaturated oleoyl chains in POPC generally reduce the bilayer hydrophobic forces relative to those exhibited by saturated assemblies at a given temperature, Figures 7 and 8 compare the intra- and intermolecular order of the two systems at temperatures for which the bilayers generally reflect the same gel and liquid-crystalline environmental effects. In the gel state the intramolecular disorder for the two bilayer assemblies remains the same to ~10 °C below their respective values for T_m, at which point the POPC bilayers begin to exhibit greater disorder (Figure 7). For the liquid-crystalline state the POPC bilayers possess a significantly greater population of chain gauche rotamers than the DMPC bilayers. As indicated in the set of temperature profiles reflecting interchain disorder in Figure 8, the POPC bilayers display an *increase in lateral order* in both the gel and liquid-crystalline phases, as compared to the DMPC system.

Although the time scales of vibrational studies and deuterium nuclear magnetic (^{2}H NMR) experiments differ considerably with rates of motion of the order of 10^{13} and 10^5 s^{-1}, respectively, it is of interest to compare the Raman results for saturated and unsaturated bilayers to the ^{2}H NMR comparisons for DPPC and POPC dispersions. In particular, Seelig & Seelig (1977) compare the hydrocarbon segmental order parameters for POPC and DPPC at a specific temperature, T_m + 19 °C, in the liquid-crystalline phase of both systems. The order parameters are close in magnitude to one another both at the beginning of the chain down to the fourth carbon atom and also from the tenth carbon atom to the end of the chain. In the middle of the chain, however, the unsaturated system is definitely more ordered, probably as a consequence of a local rigidity induced in the adjacent saturated chain by the 9,10-cis double bond (Seelig & Seelig, 1977). Since the vibrational data yield an average order integrated over the entire chain, the effect upon the entire POPC matrix from the ordering associated with the intermediate regions of the POPC chains is sufficiently strong such that the Raman spectra reflect an overall increase in interchain interactions in comparison with those of the DMPC bilayers. Despite the additional

lateral interactions arising within the POPC bilayer, the comparison with DMPC, particularly above T_m, indicates that the population of acyl chain gauche rotamers is greater at equivalent temperatures relative to the phase transition in the monounsaturated system (Figure 7). This notion is consistent with the general effect of a cis double bond inducing intramolecular chain disorder into the bilayer matrix (Seelig & Seelig, 1977); that is, the presence of a double bond lowers the barriers to rotation of the adjacent methylene units by ~40% (Flory, 1969).

The intrinsic intermolecular disorder exhibited by DMPC bilayers, in comparison to the POPC system, suggests that both lipid self-diffusion and diffusion of an integral membrane component would be easier in the DMPC liquid-crystalline state. Evidence for differences in the lateral diffusion coefficients for fluorescent lipid analogues in bilayer systems composed of saturated and unsaturated hydrocarbon chains is found, for example, in measurements involving fluorescent recovery after photobleaching procedures. In particular, the lateral diffusion coefficient of the probe molecule *N*-(4-nitrobenz-2-oxa-1,3-diazolyl)phosphatidylethanolamine is a factor of 2 greater in DMPC at 30 °C ($D = 8 \times 10^{-8}$ cm^2/s) than for the unsaturated egg yolk phosphatidylcholine bilayer system at 25 °C ($D = 4 \times 10^{-8}$ cm^2/s) (Wu et al., 1977). For a pyrene lecithin probe molecule, the lateral diffusion coefficient is ~9 times greater in a dipalmitoylphosphatidylcholine liquid-crystalline bilayer at 55 °C (T_m = 41 °C) than in an unsaturated, liquid-crystalline dioleoylphosphatidylcholine bilayer at 10 °C (T_m = −22 °C) (Galla et al., 1979). Since the lateral diffusion coefficients of membrane proteins (D_p) and lipids (D_L) are related by $D_p = (M_L/M_P)^{1/2}D_L$, where M_L and M_P represent the molecular weights of the lipids and proteins, respectively, the proteins would probably be more mobile in the lattice composed of saturated lipids, thus leading to further disruption of the lateral lipid–lipid organization (Galla et al., 1979). This reduced constraint allowing freer protein motion in saturated chain bilayer systems may account for the demonstrated difference between the DMPC and POPC bilayer perturbations induced by the Folch-Pi apoprotein.

Conclusions

In the present study we emphasize the difference in behavior between saturated and unsaturated phospholipid bilayer recombinants with myelin proteolipid apoprotein prepared in an aqueous solution. That is, the Folch-Pi apoprotein significantly perturbs the saturated DMPC bilayer lipid, while only a slight perturbation arises with the unsaturated POPC liposomes. We compare these results to the bilayer perturbations induced by the apoprotein extracted from an organic solvent medium. Thus, the variations in the temperature profiles derived from Raman spectroscopic data between those of Curatolo et al. (1978) and those presented here probably originate in the different physical and chemical properties assumed by the apoprotein in the two solvent systems (Nicot et al., 1973; Nguyen Le et al., 1976; Lavialle et al., 1979). In particular, molecular weight determinations from ultracentrifuge experiments suggest values from 64 000 to 80 000 for the apoprotein in aqueous solutions (Lavialle et al., 1979), while a value of ~25 000 is expected for the apoprotein in chloroform–methanol mixtures.

Both the physical properties of the apoprotein and the diffusion characteristics of the lipid matrix may also be factors in the differences between the temperature profiles for the recombinants involving unsaturated bilayer systems observed here and by Curatolo et al. (1978) and Verma et al. (1980). Raman temperature curves for the apoprotein delipidated with chloroform–methanol mixtures exhibited a 35 °C broadening of the transition temperature for egg yolk lecithin (Curatolo et al., 1978), as well as a broadening of the main transition in dioleoyllecithin (Verma et al., 1980). The temperature profiles in these two studies also showed discontinuities at higher temperatures which may be indicative of the melting of immobilized boundary lipid about the intrinsic membrane component (Lavialle et al., 1980). In the present study involving unsaturated POPC bilayers, the aqueous apoprotein, which exhibits a molecular weight of 64 000–80 000, only slightly depresses T_m, while broadening the phase transition by ~5 °C. Neither the DMPC nor the POPC temperature profiles involving the aqueous protein present vibrational evidence (within the precision of the experiment) for a higher temperature order–disorder transition which could be associated with a fluidization of boundary lipids.

Acknowledgments

We are extremely grateful to Dr. C. Nicot for preparing the Folch-Pi apoprotein in aqueous solution.

References

Boggs, J. M., & Moscarello, M. A. (1978) *Biochemistry 17*, 5734.

Boggs, J. M., Vail, W. J., & Moscarello, M. A. (1976) *Biochim. Biophys. Acta 448*, 517.

Boggs, J. M., Wood, D. D., Moscarello, M. A., & Papahadjopoulos, D. (1977) *Biochemistry 16*, 2325.

Bunow, M., & Levin, I. W. (1977) *Biochim. Biophys. Acta 487*, 388.

Chan, D. S., & Lees, M. B. (1974) *Biochemistry 13*, 2704.

Craig, N. C., & Levin, I. W. (1979) *Appl. Spectrosc. 33*, 475.

Curatolo, W., Sakura, J. D., Small, D. M., & Shipley, G. G. (1977) *Biochemistry 16*, 2313.

Curatolo, W., Verma, S. P., Sakura, J. D., Small, D. M., Shipley, G. G., & Wallach, D. F. H. (1978) *Biochemistry 17*, 1802.

Flory, P. J. (1969) *Statistical Mechanics of Chain Molecules*, Interscience, New York.

Folch-Pi, J., & Lees, M. B. (1951) *J. Biol. Chem. 191*, 807.

Gaber, B. P., & Peticolas, W. L. (1977) *Biochim. Biophys. Acta 465*, 260.

Galla, H.-J., Hartman, W., Theilen, U., & Sackmann, E. (1979) *J. Membr. Biol. 48*, 215.

Lavialle, F., deForesta, B., Vacher, M., Nicot, C., & Alfsen, A. (1979) *Eur. J. Biochem. 95*, 561.

Lavialle, F., Levin, I. W., & Mollay, C. (1980) *Biochim. Biophys. Acta 600*, 62.

Lees, M. B., Sakura, J. D., Sapirstein, V. S., & Curatolo, W. (1979) *Biochim. Biophys. Acta 559*, 209.

Nguyen Le, T., Nicot, C., Alfsen, A., & Baratt, M. D. (1976) *Biochim. Biophys. Acta 427*, 44.

Nicot, C., Nguyen Le, T., Lepretre, M., & Alfsen, A. (1973) *Biochim. Biophys. Acta 322*, 109.

Oldfield, E., Gilmore, R., Glaser, M., Gutowsky, H. S., Hshung, J. C., Kang, S. Y., King, T. E., Meadows, M., & Rice, D. (1978) *Proc. Natl. Acad. Sci. U.S.A. 75*, 4657.

Rice, D. M., Meadows, M. D., Scheinman, A. O., Goñi, F. M., Gômez-Fernândez, J. C., Moscarello, M., Chapman, D., & Oldfield, E. (1979a) *Biochemistry 18*, 5893.

Rice, D. M., Hsung, I. C., King, T. E., & Oldfield, E. (1979b) *Biochemistry 18*, 5885.

Seelig, A., & Seelig, J. (1977) *Biochemistry 16*, 47.

Seelig, A., & Seelig, J. (1978) *Hoppe-Seyler's Z. Physiol. Chem., Suppl. 359*, 1747.

Sherman, G., & Folch-Pi, J. (1970) *J. Neurochem. 17*, 597.
Spiker, R. C., & Levin, I. W. (1976) *Biochim. Biophys. Acta 455*, 560.
Verma, S. P., Wallach, D. F. H., & Sakura, J. D. (1980) *Biochemistry 19*, 574.
Wu, E.-S., Jacobsin, K., & Papahadjopoulous, D. (1977) *Biochemistry 16*, 3936.
Yellin, N., & Levin, I. W. (1977a) *Biochemistry 16*, 642.
Yellin, N., & Levin, I. W. (1977b) *Biochim. Biophys. Acta 489*, 177.

Comparative Lateral Diffusion of Fluorescent Lipid Analogues in Phospholipid Multibilayers†

Zenon Derzko‡ and Kenneth Jacobson*,‡

ABSTRACT: The method of fluorescence recovery after photobleaching (FRAP) has been used to measure the lateral diffusion coefficient (D) of the following fluorescent lipid probes in lipid multibilayers: carbocyanine dyes with fatty acid chains varying from 6 to 18 carbon atoms; fluorescently labeled phosphatidylcholine, phosphatidylethanolamine, and lysophosphatidylethanolamine; and fluorescently labeled fatty acid derivatives. Measurements were made in dimyristoylphosphatidylcholine (DMPC), dipalmitoylphosphatidylcholine (DPPC), brain phosphatidylserine (PS), and egg phosphatidylcholine (EPC) multibilayers. In the fluid state ($T > T_m$), the diffusion coefficients are relatively insensitive to the structure of the lipid analogue, probably because, if the probe is disposed as an amphipath, its motion depends on the self-diffusion of the host bilayer lipids. The activation energy for the diffusion of most lipid analogues was between 4 and 8 kcal/mol. Significant differences in the lateral diffusion of the analogues were found when bilayers of different composition were compared at the same reduced temperature. Diffusion in longer chain natural phospholipid (EPC, PS) bilayers was significantly slower than in shorter chain saturates (DMPC, DPPC). On the other hand, diffusion in DPPC bilayers was faster than in DMPC membranes which correlates with the greater lateral expansion of DPPC compared to DMPC bilayers above their respective transitions [Janiak, M., Small, D., & Shipley, C. G. (1979) *J. Biol. Chem. 254*, 6068]. Below the transition temperature of DMPC and PS multibilayers, the FRAP kinetics are generally best fitted by two diffusion coefficients. The slow component ($D \leq 5 \times 10^{-11}$ cm^2/s) may be true bulk gel-phase lateral diffusion while the fast component ($10^{-10} < D \lesssim 10^{-8}$ cm^2/s) may be associated with transport along numerous defects apparent in the gel phase. The proportion of fast and slow diffusing probe depends on the structure of the lipid analogue and the chromophore.

The fluorescence recovery after photobleaching (FRAP)[1] technique for measuring the mobility of various fluorescent membrane associated molecules has become a more common experimental procedure. A number of studies have been carried out on lipid and protein diffusion in model membrane systems and directly on single living cells [for review, see Cherry (1979); Jacobson (1980)]. The model-system studies can be used to assist in the interpretation of the results obtained from the cell surface. Recently, fluorescent lipid diffusion has been investigated in multibilayers (Wu et al., 1977; Fahey & Webb, 1978; Smith & McConnell, 1978; Rubenstein et al., 1979), unilamellar vesicles (Fahey & Webb, 1978), and black lipid membranes (Fahey & Webb, 1978). Peptides (Wu et al., 1978), stearoylated dextrans (Wolf et al., 1977), and proteins (Derzko & Jacobson, 1978; Vaz et al., 1978; Smith et al., 1979) have been incorporated into lipid membranes and their diffusions measured.

The purpose of this work was to further study the dependence of lipid analogue diffusion on molecular size and shape in multibilayers composed of several different phospholipids. Comparisons of the diffusion of various probes were made in multibilayers in both the liquid crystalline and the gel phases. A light microscopic study of bilayers undergoing the gel to liquid-crystalline phase transition is also presented.

Materials and Methods

Preparation of Lipids. The phospholipids used in this study were isolated or synthesized by Mr. T. Isac in the laboratory of Dr. D. Papahadjopoulos and contained no detectable impurities as determined by thin-layer chromatography on silica gel H and a solvent of chloroform/methanol/7 M ammonia

† From the Department of Experimental Pathology, Roswell Park Memorial Institute, Buffalo, New York 14263 (K.J.), and the Department of Biophysical Sciences, State University of New York at Buffalo, Buffalo, New York 14226 (Z.D.). *Received March 7, 1980; revised manuscript received July 23, 1980.* This work was supported by Grant CA-16743 awarded by the National Institutes of Health, Department of Health, Education and Welfare. This work was submitted by Z.D. in partial fulfillment of the requirements for the Ph.D. degree at the State University of New York in Buffalo, NY 14226. K.J. is an Established Investigator of the American Heart Association. A preliminary account of this work was presented to the 1979 Biophysical Society Meeting (Derzko & Jacobson, 1979).

‡ Present address: Laboratories for Cell Biology, Department of Anatomy, University of North Carolina, Chapel Hill, NC 27514.

[1] Abbreviations used: DMPC, dimyristoylphosphatidylcholine; DPPC, dipalmitoylphosphatidylcholine; PS, phosphatidylserine; EPC, egg phosphatidylcholine; NBD-PE, *N*-(4-nitrobenzo-2-oxa-1,3-diazolyl)-phosphatidylethanolamine; NBD-PC, 1-acyl-2-[*N*-(4-nitrobenzo-2-oxa-1,3-diazolyl)aminocaproyl]phosphatidylcholine; NBD-lysoPE, *N*-(4-nitrobenzo-2-oxa-1,3-diazolyl)lysophosphatidylethanolamine; NBD-C_{12}, 12-[methyl(7-nitrobenz-2-oxa-1,3-diazol-4-yl)amino]dodecanoic acid; F-C_{16}, 5-(hexadecanoylamino)fluorescein; F-C_{14}, 5-(tetradecanoylamino)fluorescein; diO-C_{18}(3), 3,3′-dioctadecyloxacarbocyanine iodide; diO-C_{14}(3), 3,3′-ditetradecyloxacarbocyanine iodide; diO-C_{10}(3), 3,3′-didecanoyloxacarbocyanine iodide; diO-C_6(3), 3,3′-dihexyloxacarbocyanine iodide; diI-C_{18}(3), 3,3′-dioctadecylindocarbocyanine iodide; diI-C_{16}(3) 3,3′-dihexadecylindocarbocyanine iodide; diI-C_{12}(3),3,3′-didodecanoylindocarbocyanine iodide; T_m, gel to liquid crystalline phase transition temperature; FRAP, fluorescence recovery after photobleaching; % R, percent recovery; $\tau_{1/2}$, half-time for recovery; w_s, laser spot radius at specimen plane; T_B, time of photobleaching; I_B, photobleaching intensity; D, diffusion coefficient.

0006-2960/80/0419-6050$01.00/0